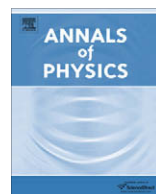




Contents lists available at ScienceDirect

## Annals of Physics

journal homepage: [www.elsevier.com/locate/aop](http://www.elsevier.com/locate/aop)

# Dynamics of interface in three-dimensional anisotropic bistable reaction–diffusion system

Zhi Zhu He<sup>a</sup>, Jing Liu<sup>a,b,\*</sup><sup>a</sup> Key Laboratory of Cryogenics, Technical Institute of Physics and Chemistry, Chinese Academy of Sciences, Beijing 100190, China<sup>b</sup> Department of Biomedical Engineering, School of Medicine, Tsinghua University, Beijing 100084, China

## ARTICLE INFO

*Article history:*

Received 7 July 2009

Accepted 12 October 2009

Available online 14 October 2009

*Keywords:*

Dynamics of interface

Reaction–diffusion

Chemical front

Anisotropic bistable media

## ABSTRACT

This paper presents a theoretical investigation of dynamics of interface (wave front) in three-dimensional (3D) reaction–diffusion (RD) system for bistable media with anisotropy constructed by means of anisotropic surface tension. An equation of motion for the wave front is derived to carry out stability analysis of transverse perturbations, which discloses mechanism of pattern formation such as labyrinthine in 3D bistable media. Particularly, the effects of anisotropy on wave propagation are studied. It was found that, sufficiently strong anisotropy can induce dynamical instabilities and lead to breakup of the wave front. With the fast-inhibitor limit, the bistable system can further be described by a variational dynamics so that the boundary integral method is adopted to study the dynamics of wave fronts.

© 2009 Elsevier Inc. All rights reserved.

## 1. Introduction

Reaction–diffusion systems such as chemical reactions or electrical action potential propagation in cardiac tissue exhibit a variety of spatiotemporal patterns due to the coupling of non-linear reaction kinetics and diffusion of species [1]. One of the most prominent chemical systems is iodate–ferrocyanide–sulfite (FIS) reaction, where rich patterns, such as labyrinthine, spot replication, and spiral wave turbulence, have been observed in numerical simulations and experiments [2]. FIS is a typical bistable RD system, which is composed of two states in different regions separated by front structures (called interface) across which the chemical concentrations change sharply. The global behaviour of pattern

\* Corresponding author. Address: Technical Institute of Physics and Chemistry, Key Laboratory of Cryogenics, Chinese Academy of Sciences, Beijing 100190, China. Tel.: +86 10 82543765; fax: +86 10 82543767.

E-mail address: [jliu@mail.ipc.ac.cn](mailto:jliu@mail.ipc.ac.cn) (J. Liu).

formation strongly depends on the fronts' inner structure [3]. Two front instabilities in bistable system, an instability to transverse perturbations and a non-equilibrium Ising–Bloch (NIB) front bifurcation [4], have been developed to explain formation of complex patterns. With the fast-inhibitor limit, a non-local contour dynamics model [5,6] for interface motion has been developed in two-dimensional isotropic bistable system to study pattern evolution far beyond the linear instability of localized states.

A realistic media is often anisotropic, which may be induced by intrinsic inhomogeneity of media [7]. Some novel phenomena unobservable in isotropic systems, such as reaction diffusion waves with sharp corners [8], and traveling wave fragments along a preferred orientation and stratified spatio-temporal chaos characterized by strong correlations along principal direction [9], have been discovered in anisotropic media. For an anisotropic bistable media, the normal velocity of chemical wave depends on its propagation direction. A constant anisotropic diffusion coefficient tensor can be easily removed from the reaction diffusion equation by rescaling the spatial coordinates, while a complex anisotropy, such as state-dependent anisotropy, cannot be eliminated by such transformation. Recently, a general anisotropy expression [7,10] is absorbed to two-dimensional RD system, which is similar to that in crystal growth [11,12]. This method effectively characterizes the effects of anisotropy on the pattern formation and can be used to predict the anisotropy induced new chemical wave pattern formation such as polygon-shaped patterns (typical triangular, rectangular target wave and spiral wave [13–16]) and then study related dynamical mechanism.

The FitzHugh–Nagumo (FHN) models considering anisotropy are adopted as follows [7]:

$$\begin{cases} \partial_t u = D_u \nabla \cdot \left\{ \frac{1}{2} \partial_{\partial_t u} \left[ |\nabla u|^2 \gamma^2(v) \right] \right\} + \varepsilon_u (u - u^3 - v) \\ \partial_t v = D_v \nabla^2 v + \varepsilon_v (u - a_1 v - a_0) \end{cases}, \quad (1)$$

where  $u$  and  $v$  represent the activator and the inhibitor. The homogenous function  $\gamma(\lambda v) = \lambda \gamma(v)$  is dimensionless anisotropy function with  $v = \nabla u / |\nabla u|$ . For the classical diffusion tensor  $\mathbf{D}$ ,  $\gamma$  can reduce to  $|\nabla u| \gamma(v) = \sqrt{[\nabla u]^T \cdot \mathbf{D} \cdot [\nabla u]}$  so that Eq. (1) can be reduced to the classical anisotropic model. Many interesting patterns, such as lamellar, hexagonal, spherical [17] and knotted labyrinthine patterns [18] have been observed in 3D isotropic system. Although isotropic 2D bistable media described by Eq. (1) has been extensively investigated, the pattern formation in 3D bistable system, particularly, considering the effects of anisotropy, has been less studied so far. The purpose of this paper is to investigate the dynamics of chemical front in 3D anisotropic bistable media. An equation of motion for the wave front is firstly derived so that stability analysis of transverse perturbations is discussed and the effects of anisotropy on wave propagation are studied. It is found that sufficiently strong anisotropy can induce dynamical instabilities and lead to breakup of the wave front. With the fast-inhibitor limit, the bistable system can be described by a variational dynamics so that the boundary integral method [5] is adopted to study the dynamics of 3D wave fronts, which results in an fully non-local and an approximate local interface motion dynamics equations.

## 2. Velocity curvature relation and transverse instability of planar fronts

By setting  $t = \varepsilon_v t$  and  $x = \sqrt{\varepsilon_v / D_v} x$ , Eq. (1) can be expressed as dimensionless form as

$$\begin{cases} \partial_t u = \beta^{-1} \nabla \cdot \left\{ \frac{1}{2} \partial_{\partial_t u} \left[ |\nabla u|^2 \gamma^2(v) \right] \right\} + \varepsilon^{-1} (u - u^3 - v) \\ \partial_t v = \nabla^2 v + (u - a_1 v - a_0) \end{cases}, \quad (2)$$

where  $\beta = D_v / D_u$  denotes ratio between diffusion coefficient of  $(u, v)$ ;  $\varepsilon = \varepsilon_v / \varepsilon_u$  characterizes the time scales associated with evolution of  $u$  and  $v$ ;  $a_1$  and  $a_0$  are prescribed proper values for a bistable media with a double well structure. A singular perturbation approach is adopted to obtain velocity–curvature relations, which is valid for the small parameter  $\mu = \sqrt{\varepsilon / \beta} \ll 1$ . It is convenient to introduce a local moving orthogonal coordinate system

$$\mathbf{r} = \mathbf{R}(\xi^1, \xi^2, t) + r \mathbf{e}_3(\xi^1, \xi^2), \quad (3)$$

where,  $\mathbf{r}$  is the position vector of a point near the wave front,  $\mathbf{R}$  represents the position of the wave front,  $\mathbf{e}_3$  is the unit normal vector of the interface, and  $\xi^i$  ( $i = 1, 2$ ) is corresponding to arc length along the principal curvatures of the interface. Then the unit tangent vectors of the interface are given as  $\mathbf{e}_i = \partial_{\xi^i} \mathbf{R}$ . The derivatives of the normal vector are described as  $\partial_{\xi^i} \mathbf{e}_3 = \kappa_i \mathbf{e}_i$ , where  $\kappa_i$  is the principal curvatures of the interface. Another coordinate on the interface can be obtained by  $\partial_{\xi^i} \xi^i = \kappa_i$ , which will be convenient for following derivation. It is now easy to describe the local moving orthogonal coordinate basis vectors in

$$\mathbf{n} = \partial_r \mathbf{r} = \mathbf{e}_3, \quad \mathbf{e}_{\xi^1} = \partial_{\xi^1} \mathbf{r} = (1 + r\kappa_1) \mathbf{e}_1, \quad \mathbf{e}_{\xi^2} = \partial_{\xi^2} \mathbf{r} = (1 + r\kappa_2) \mathbf{e}_2. \quad (4)$$

For  $\mu = \sqrt{\varepsilon/\beta} \ll 1$ , the narrow regions along the normal to wave front, where  $\partial_r u \approx O(\mu^{-1})$  and  $\partial_r v \approx O(1)$ , are considered as fronts' inner regions, while both  $\partial_r u$  and  $\partial_r v$  are of order unity in outer regions. The dynamics in the inner regions is studied by introducing a stretched normal coordinate  $\rho = r/\mu$ , with corresponding expansions

$$\begin{aligned} u(r, \xi^i, t) &= u^{(0)}(\rho, \xi^i, t) + \mu u^{(1)}(\rho, \xi^i, t) + \mu^2 u^{(2)}(\rho, \xi^i, t) + \cdots, \\ v(r, \xi^i, t) &= v^{(0)}(\rho, \xi^i, t) + \mu v^{(1)}(\rho, \xi^i, t) + \mu^2 v^{(2)}(\rho, \xi^i, t) + \cdots. \end{aligned} \quad (5)$$

The time derivative now becomes

$$\partial_t u = \partial_t u^{(0)} - V_n \partial_\rho u^{(0)} + \xi^i \partial_{\xi^i} u^{(0)} + O(\mu), \quad (6)$$

where  $\xi^i = \partial_t \xi^i$  and  $V_n = -\partial_t \rho$  is the front velocity in a direction normal to the wave front. It is easy to find that

$$-\frac{\nabla u}{|\nabla u|} = -\frac{\mathbf{n}\mu^{-1}\partial_\rho u + \mathbf{e}_{\xi^i}\partial_{\xi^i} u}{|\mathbf{n}\mu^{-1}\partial_\rho u + \mathbf{e}_{\xi^i}\partial_{\xi^i} u|} = \mathbf{n} + \mathbf{e}_i \mu \frac{\partial_{\xi^i} u}{\partial_\rho u} + O(\mu^2), \quad (7)$$

where we assume that  $u^{(0)} < 0$  (see Eq. (13)). Then we can obtain the relation

$$|-\nabla u|^2 \gamma^2 \left( -\frac{\nabla u}{|\nabla u|} \right) = \mu^{-2} (\tilde{\gamma} \partial_\rho u)^2 + \mu^{-1} \partial_\rho u \partial_{\xi^i} u \partial_{\xi^i} \tilde{\gamma}^2 + O(1), \quad (8)$$

where  $\tilde{\gamma} = \tilde{\gamma}(\mathbf{n})$ . We assume  $\mathbf{A} = A_\rho \mathbf{n} + A_{\xi^i} \mathbf{e}_{\xi^i}$ , which satisfies

$$\nabla \cdot \mathbf{A} = \nabla \cdot \left\{ \frac{1}{2} \partial_{\partial_t u} \left[ |-\nabla u|^2 \gamma^2 \left( -\frac{\nabla u}{|\nabla u|} \right) \right] \right\}. \quad (9)$$

Comparing Eq. (8) with Eq. (9), one can find by

$$\begin{aligned} A_\rho &= \mu^{-1} \tilde{\gamma}^2 \partial_\rho u + \frac{1}{2} \partial_{\xi^i} \tilde{\gamma}^2 \partial_{\xi^i} u + O(\mu) = \mu^{-1} \tilde{\gamma}^2 \partial_\rho u^{(0)} + \tilde{\gamma}^2 \partial_\rho u^{(1)} + \frac{1}{2} \partial_{\xi^i} \tilde{\gamma}^2 \partial_{\xi^i} u^{(0)} + O(\mu) \\ A_{\xi^i} &= \frac{1}{2} \mu^{-1} \partial_{\xi^i} \tilde{\gamma}^2 \partial_\rho u + O(1) = \frac{1}{2} \mu^{-1} \partial_\rho u^{(0)} \partial_{\xi^i} \tilde{\gamma}^2 + O(1). \end{aligned} \quad (10)$$

The expansion of the diffusion term is finally described by

$$\begin{aligned} \nabla \cdot \mathbf{A} &= \mu^{-1} \left( \partial_\rho A_\rho + A_r \frac{1}{\sqrt{g}} \partial_\rho \sqrt{g} \right) + \left( \partial_{\xi^i} A_{\xi^i} + \frac{1}{\sqrt{g}} A_{\xi^i} \partial_{\xi^i} \sqrt{g} \right) \\ &= \mu^{-2} \tilde{\gamma}^2 \partial_{\rho\rho} u^{(0)} + \mu^{-1} \tilde{\gamma}^2 \partial_\rho u^{(1)} + \mu^{-1} \partial_{\xi^i} \tilde{\gamma}^2 \partial_{\rho \xi^i} u^{(0)} + \mu^{-1} \left[ (\kappa_1 + \kappa_2) \tilde{\gamma}^2 + \frac{1}{2} \partial_{\xi^i \xi^i} \tilde{\gamma}^2 \right] \partial_\rho u^{(0)} \\ &\quad + O(1), \end{aligned} \quad (11)$$

where we have used  $\sqrt{g} = 1 + \mu\rho(\kappa_1 + \kappa_2) + O(\mu^2)$ . The expansion of reaction term is given by

$$u - u^3 - v = \left[ u^{(0)} - (u^{(0)})^3 - v_f^{(0)} \right] + \mu \left[ 1 - 3(u^{(0)})^2 \right] u^{(1)} + \mu v_f^{(1)} + O(\mu^2). \quad (12)$$

The leading order stationary wave front solution is found by

$$u^{(0)} = -\tanh\left(\frac{\rho}{\tilde{\gamma}\sqrt{2}}\right), \quad v_f^{(0)} = 0. \quad (13)$$

The first order solution is given by

$$Lu^{(1)} = \eta(u_t^{(0)} - V_n \partial_\rho u^{(0)} + \xi^i \partial_{\xi^i} u^{(0)} + v_f^1) - \partial_{\xi^i} \tilde{\gamma}^2 \partial_{\rho \xi^i} u^{(0)} - \left[ (\kappa_1 + \kappa_2) \tilde{\gamma}^2 + \frac{1}{2} \partial_{\xi^i \xi^i} \tilde{\gamma}^2 \right] \partial_\rho u^{(0)}, \quad (14)$$

where  $L = \tilde{\gamma}^2 \partial_{\rho\rho} + [1 - 3(u^{(0)})^2]$ . Since  $Lu_\rho^{(0)} = 0$ , Eq. (14) must satisfy the solvability followed by:

$$\begin{aligned} \eta V_n \int_{-\infty}^{+\infty} (\partial_\rho u^{(0)})^2 d\rho &= \int_{-\infty}^{+\infty} v_f^1 \partial_\rho u^{(0)} d\rho + \int_{-\infty}^{+\infty} \eta (\partial_\tau u^{(0)} + \xi^i \partial_{\xi^i} u^{(0)}) \partial_\rho u^{(0)} d\rho \\ &\quad - \left[ (\kappa_1 + \kappa_2) \tilde{\gamma}^2 + \frac{1}{2} \partial_{\xi^i \xi^i} \tilde{\gamma}^2 \right] \int_{-\infty}^{+\infty} (\partial_\rho u^{(0)})^2 d\rho \\ &\quad - \frac{1}{2} \partial_{\xi^i} \tilde{\gamma}^2 \partial_{\xi^i} \left[ \int_{-\infty}^{+\infty} \left( \frac{\partial u^{(0)}}{\partial \rho} \right)^2 d\rho \right]. \end{aligned} \quad (15)$$

According to Eq. (13), Eq. (15) can be reduced to

$$C_n = -\frac{3\tilde{\gamma}}{\sqrt{2}\eta} v_f - \delta^{-1} \tilde{\gamma} [\tilde{\gamma}(\kappa_1 + \kappa_2) + \tilde{\gamma}_{ani}], \quad (16)$$

where  $V_n = \mu C_n$ ,  $v_f^1 = \mu v_f + O(\mu^2)$ ,  $\eta = \sqrt{\varepsilon\beta}$  and  $\tilde{\gamma}_{ani} = \kappa_1 \partial_{\xi^1 \xi^1} \tilde{\gamma} + \kappa_2 \partial_{\xi^2 \xi^2} \tilde{\gamma}$ . For outer regions, the relation between  $v_f$  and  $C_n$  [9] also can be found by

$$v_f = -\frac{C_n + \kappa_1 + \kappa_2}{q^2 \sqrt{(C_n + \kappa_1 + \kappa_2)^2 + 4q^2}} - \frac{a_0}{q^2}, \quad (17)$$

where  $q^2 = a_1 + 1/2$ . An implicit relation between the normal velocity of the front and its curvature is therefore deduced from Eqs. (16) and (17) by

$$C_n + \beta^{-1} \tilde{\gamma} [\tilde{\gamma}(\kappa_1 + \kappa_2) + \tilde{\gamma}_{ani}] = \frac{3\tilde{\gamma}}{\eta\sqrt{2}} \left[ \frac{C_n + \kappa_1 + \kappa_2}{q^2 \sqrt{(C_n + \kappa_1 + \kappa_2)^2 + 4q^2}} + \frac{a_0}{q^2} \right]. \quad (18)$$

Eq. (18) can be reduced to 2D case with  $\kappa_2 = 0$  [7]. For  $\tilde{\gamma} = \text{const}$ ,  $\tilde{\gamma}_{ani} = 0$  is corresponding to isotropic case.

A bistable media with two stationary and uniform stable states, an up state ( $u_+$ ,  $v_+$ ) and a down state ( $u_-$ ,  $v_-$ ), is connected by front solutions. In the symmetric system ( $a_0 = 0$ ), the planar fronts ( $\kappa_i = 0$ ) solutions are obtained from Eq. (18) with a single front (called “Ising” front) solution as  $C_0 = 0$ , and a pair counter-propagating fronts (called Bloch fronts) solutions as  $C_0 = \pm 2q\eta^{-1} \sqrt{\tilde{\gamma}^2 \eta_c^2 - \eta^2}$  for  $\eta \leq \tilde{\gamma} \eta_c$ , where  $\eta_c = 3/(2\sqrt{2}q^3)$ . The threshold of the NIB bifurcation (denoting transition between wave fronts) is found by  $\eta_c^{ani} = \eta_c \tilde{\gamma} (1 - a_0^{2/3})^{3/2}$ . An “Ising” front will lose stability to a pair of “Bloch” fronts when  $\eta$  changes from  $\eta > \eta_c$  to  $\eta \leq \eta_c$  [9]. For asymmetric system ( $a_0 \neq 0$ ),  $C_0$  is determined by

$$C_0 = \frac{3\tilde{\gamma}}{\eta\sqrt{2}} \left[ \frac{C_0}{q^2 \sqrt{C_0^2 + 4q^2}} + \frac{a_0}{q^2} \right]. \quad (19)$$

For a weakly curvature interface ( $\kappa_i \ll 1$ ), Eq. (18) can be expanded in powers of the curvature by

$$C_n = C_0 - \tilde{\gamma} \left[ (\beta^{-1} \tilde{\gamma} - \chi) + \beta^{-1} \partial_{\xi^1 \xi^1} \tilde{\gamma} \right] \kappa_1 - \tilde{\gamma} \left[ (\beta^{-1} \tilde{\gamma} - \chi) + \beta^{-1} \partial_{\xi^2 \xi^2} \tilde{\gamma} \right] \kappa_2 + O(\kappa_i^2), \quad (20)$$

where  $\chi = 6\sqrt{2}\eta^{-1} (C_0^2 + 4q^2)^{-3/2}$  and  $C_0$  is given by Eq. (19). For the isotropic case ( $\partial_{\xi^1 \xi^1} \tilde{\gamma} = \partial_{\xi^2 \xi^2} \tilde{\gamma} = 0$ ), the threshold of transverse instability occurring in front solution satisfies the relation  $\beta\chi = \tilde{\gamma}$ , which is similar to that in 2D case. The effects of the anisotropy have been studied in 2D system ( $\kappa_2 = 0$ ) [7]. However, the effects of the anisotropy perform more complex in 3D system. A spherical coordinate ( $R, \theta, \varphi$ ), where we assume  $\kappa_i = R^{-1}$ , is adopted to obtain an equation of threshold of transverse by

$$2\beta\chi = 2\tilde{\gamma} + \partial_{\theta\theta} \tilde{\gamma} + \cot \theta \partial_\theta \tilde{\gamma} + \sin^{-2} \theta \partial_{\varphi\varphi} \tilde{\gamma}. \quad (21)$$

It is noted that the left-hand side of Eq. (21) is always positive while it is hard to make sure that the right-hand side of Eq. (21) is positive, which depends on the choice of  $\tilde{\gamma}$ . For a simple anisotropy form  $\mathbf{D} = \text{diag}\{d_x, d_y, d_z\}$ , one can find  $\tilde{\gamma} = \sqrt{d_x \sin^2 \theta \cos^2 \varphi + d_y \sin^2 \theta \cos^2 \varphi + d_z \cos^2 \theta}$ . In such choice of  $\tilde{\gamma}$ , it is easy to demonstrate that the right-hand side of Eq. (21) is always positive. According to Eq. (21), the value of  $\beta\chi$  changes in different directions, which can be used to obtain NIB bifurcation and planar front transverse instability boundaries in the parameters space  $(\beta, \varepsilon)$  for all the directions. However, for a complex anisotropy, such as  $d_x$  is not constant and changes in directions [8], the right-hand side of Eq. (1) may become negative, which indicates that the propagation of chemical wave fails in the whole parameters space  $(\beta, \varepsilon)$ . It is noted that the instability of the propagation of chemical wave firstly occurs in the directions where the right-hand side of Eq. (1) is negative, which has been demonstrated in 2D case [7].

### 3. Non-local contour dynamics for interface with the fast-inhibitor limit

In the fast-inhibitor limit,  $D_v \rightarrow \infty$  with  $\varepsilon_v/D_v$  finite, Eq. (1) are rewritten as

$$\begin{cases} \partial_t u = D \nabla \cdot \left\{ \frac{1}{2} \partial_{\theta} u \left[ |\nabla u|^2 \gamma^2(v) \right] \right\} + \varepsilon_u (u - u^3 - v) \\ \nabla^2 v - a_1 v = -(u - a_0) \end{cases} \quad (22)$$

with dimensionless transformation  $t = t$ ,  $x = \sqrt{\varepsilon_v/D_v} x$  and  $D = D_u \varepsilon_v/D_v$ . Eq. (22) can be expressed in a variational form [7]

$$\partial_t u = -\frac{\delta F}{\delta u}, \quad (23)$$

and Lyapunov energy  $F$  is given as

$$F = \int d^3 r \left[ \frac{D}{2} |\nabla u|^2 \gamma^2(v) + U_0(u) + U_1(u) \right] + \frac{\varepsilon_u}{2} \int \int d^3 r d^3 r' u(\mathbf{r}) G u(\mathbf{r}'), \quad (24)$$

where  $U_0(u) = u^4/4 - u^2/2$ ,  $U_1(u) = \varepsilon_u(u^4/4 - u^2/2 + a_0 \omega^2 u) - U_0(u)$ , and 3D Green's function satisfies the relation

$$(\nabla^2 - \omega^2)G = -\delta^3(\mathbf{r} - \mathbf{r}'), \quad (25)$$

where  $G = (4\pi R)^{-1} \exp(-\omega^{-1}R)$  with  $R = |\mathbf{r} - \mathbf{r}'|$  and  $\omega = a_1^{-1/2}$ . The right-hand term of Eq. (23) is described by a variational form while the left-hand term is not in such form. A complete description by variational form may be

$$\frac{\delta R}{\delta u_t} = -\frac{\delta F}{\delta u} \quad (26)$$

where  $R = \int d^3 r u_t^2/2$ .

In order to obtain a contour dynamical equation for wave front motion described by Eq. (26), we consider a bistable media composed of a single island of  $u_{in} = 1$  surrounded by an infinite sea of  $u_{out} = 0$ . The interface of the island is determined by a hyperbolic tangent profile according to Eq. (13). From Eq. (24), it is noted that the chemical front motion is determined by the non-local Lyapunov energy, which is partitioned into three contributions  $F = F_l + F_p + F_f$ : an effective line tension, a pressure, and a non-local coupling force between fronts, particularly, described as follows. The contribution of effective surface tension is significant only in the neighborhood of the wave front where  $|\nabla u|$  is non-negligible.

$$\begin{aligned} F_l &= \int d^3 r \left[ \frac{D}{2} |\nabla u|^2 \gamma^2(v) + U_0(u) \right] = \int d^3 r D |\nabla u|^2 \gamma^2(v) = D \int_{-\infty}^{+\infty} \int_S dS dr (\partial_t u)^2 \tilde{\gamma}^2 \\ &= \gamma_0 \int_S dS \tilde{\gamma}, \end{aligned} \quad (27)$$

where  $u = -\tanh(r/\tilde{\gamma} \sqrt{2D\varepsilon_u^{-1}})$  with corresponding to Eq. (22), and  $\gamma_0 = \sqrt{2D\varepsilon_u}/3$  is effective surface tension for the isotropic case. We have used the asymptotic result that near interface  $U_0(u) \simeq \frac{D}{2} |\nabla u|^2 \gamma^2(v)$ . The contribution of pressure is proportional to the island volume

$$F_p = \int d^3r U_1(u) = [U_1(1) - U_1(0)] \int_V d^3r \quad (28)$$

According to Eq. (25), the contribution from the interaction of fronts can be reduced to

$$\begin{aligned} F_f &= \frac{\varepsilon_u}{2} \int_V \int_V d^3r d^3r' G = \frac{\varepsilon_u}{2} \int_V \int_V d^3r d^3r' \{ \omega^2 [\nabla^2 G + \delta^3(\mathbf{r} - \mathbf{r}')] \} \\ &= \frac{\varepsilon_u \omega^2}{2} \int_V d^3r - \frac{\varepsilon_u \omega^2}{2} \int_S dS \int_S dS' \mathbf{n} \cdot \mathbf{n}' G, \end{aligned} \quad (29)$$

where we have used  $\int_V d^3r \nabla G = \int_{\partial V} dS \mathbf{n} G$  and  $\nabla^2 G = -\nabla_{\mathbf{r}} \cdot \nabla_{\mathbf{r}'} G$ . Substituting Eqs. (27)–(29) to Eq. (24), one can obtain

$$F = \Delta p \int_V d^3r + \gamma_0 \int_S dS \tilde{\gamma} - \frac{\varepsilon_u \omega^2}{2} \int_S dS \int_S dS' \mathbf{n} \cdot \mathbf{n}' G, \quad (30)$$

where  $\Delta p = U_1(1) - U_1(0) + \varepsilon_u \omega^2/2$  represents an effective pressure. In terms of Eq. (6), an asymptotic result is  $u_t = -(\mathbf{r}_t \cdot \mathbf{n}) \partial_t u$  for wave front local moving coordinates such that

$$R = \frac{\tilde{\gamma}}{2D} \int_S ds (\mathbf{r}_t \cdot \mathbf{n})^2 \quad (31)$$

Eqs. (30) and (31) indicate that both  $F$  and  $R$  can be transformed as wave front ( $\mathbf{r}$  and  $\mathbf{r}_t$ ) function. A heuristic translation of Eq. (26) into variational function considering wave front may be

$$\mathbf{n} \cdot \frac{\delta R}{\delta \mathbf{r}_t} = -\mathbf{n} \cdot \frac{\delta F}{\delta \mathbf{r}} \quad (32)$$

Substituting Eqs. (30) and (31) to Eq. (32) (see Appendix A), a non-local contour dynamics equation for interface motion with the fast-inhibitor limit is finally given as

$$\mathbf{r}_t \cdot \mathbf{n} = -\frac{D\tilde{\gamma}}{\gamma_0} \left\{ \Delta p + \gamma_0 \Delta \tilde{\gamma} - \frac{1}{2} \varepsilon_u \omega^2 \int_S dS' \frac{\mathbf{e}_2' \cdot [(\mathbf{r} - \mathbf{r}') \wedge \mathbf{e}_1']}{|\mathbf{r} - \mathbf{r}'|} \frac{dG}{dR} \right\}, \quad (33)$$

where  $\Delta \tilde{\gamma} = \tilde{\gamma}(\kappa_1 + \kappa_2) + \tilde{\gamma}_{ani}$  (see Appendix A).

For  $\omega \kappa_i \ll 1$ , an approximate local dynamics [5] based on Eq. (30) can be found. It is noted that the contribution to the double integral in Eq. (30) is mainly from the domain  $|\mathbf{r} - \mathbf{r}'| \leq \omega$  so that it is first approximately evaluated by  $\mathbf{r}'$  integral over the whole tangent plane of interface

$$\int_S dS \int_S dS' \mathbf{n} \cdot \mathbf{n}' G = \frac{\omega}{2} \int_S dS \left[ 1 - \frac{1}{2} \omega^2 (3H^2 - K) + O((\omega \kappa_i)^4) \right], \quad (34)$$

where  $H = (\kappa_1 + \kappa_2)/2$  is the mean curvature and  $K = \kappa_1 \kappa_2$  is the Gaussian curvature (see Appendix B). Substituting Eq. (34) to Eq. (30), one can obtain

$$F = \Delta p \int_V d^3r + \int_S dS [(\gamma_0 \tilde{\gamma} - 2\gamma_c) + \gamma_c \omega^2 (3H^2 - K)], \quad (35)$$

where  $\gamma_c = \varepsilon_u \omega^3/8$ . An approximate local dynamics is obtained by the functional derivative of  $F$  (see Appendix A)

$$\mathbf{r}_t \cdot \mathbf{n} = -\frac{D\tilde{\gamma}}{\gamma_0} [\Delta p + \gamma_0 \Delta \tilde{\gamma} - 4\gamma_c H + 3\gamma_c \omega^2 (\Delta_s H + 2H^3 - 2HK)], \quad (36)$$

where the effective surface tension can be considered as  $\gamma_0 \Delta \tilde{\gamma} - 4\gamma_c H$ . A linear stability analysis of sphere shape is easily obtained according to Eq. (36). Comparing Eq. (18) with Eq. (36), one can find that the form of the term for anisotropic surface tension is equal. It is noteworthy that the last terms at right-hand side of Eq. (36) is derived from  $H^2$  (See Appendix A or detailed in Ref. [19]). Eq. (36) is similar to a geometrical model [20] developed to describe the interface evolution, where an additional curvature dependent energy  $H^2$  is absorbed to surface energy.

#### 4. Conclusion

In summary, the present paper has investigated dynamics of chemical front in 3D bistable media with anisotropy constructed by means of anisotropic surface tension. A velocity curvature relation for 3D chemical fronts has been obtained and transverse instability of planar fronts was studied. Particularly, the effects of anisotropy on chemical wave propagation have been demonstrated, such as sufficiently strong anisotropy would induce the dynamical instabilities and lead to breakup of the chemical wave. We also obtained two equations regarding anisotropy for 3D case, a fully non-local interface motion equation and an approximate local interface motion equation, by means of the boundary integral method. Possible extensions include studying spatial inhomogeneous anisotropy, and the applications of these methods to electrical action potential propagation in anisotropic 3D cardiac tissue (excitable media). The notation of anisotropy function can also be extended to study the influence of anisotropy on dynamics of interface in Type-1 superconductors, magnetic fluids or Langmuir monolayer [5,21].

#### Acknowledgment

This work is partially supported by the National Natural Science Foundation of China under grant 50776097 and Tsinghua-Yue-Yuen Medical Sciences Fund.

#### Appendix A

Here we give the functional derivatives from Eqs. (33) and (36) by using the Euler–Lagrange equations. We firstly assume  $\delta \mathbf{r} = \mathbf{n} \delta r$ . Then it is noted that relations

$$\delta(dS) = 2H\delta r dS, \quad \delta \mathbf{n} = -\nabla_s \delta r, \quad (\text{A1})$$

where  $\nabla_s = \mathbf{e}_i \partial_{\zeta_i}$ . It is easy to obtain the volume and surface derivation

$$\delta \int_V d^3r = \int_S dS \delta r, \quad \delta \int_S dS = \int_S dS 2H \delta r. \quad (\text{A2})$$

The functional derivatives of  $F_f$  can be given as

$$\begin{aligned} \delta \int_S dS \mathbf{n}' \cdot \mathbf{n} G &= \int_S dS [\mathbf{n}' \cdot (G \delta \mathbf{n} + \mathbf{n} \delta G) + \mathbf{n}' \cdot \mathbf{n} G (\nabla_s \cdot \mathbf{n}) \delta r] \\ &= \int_S dS [\mathbf{n}' \cdot (-G \nabla_s \delta r + \mathbf{n} \delta G) - \mathbf{n} \cdot (\nabla_s \mathbf{n}' \cdot \mathbf{n} G) \delta r] = \int_S dS \mathbf{n}' \cdot (\delta r \nabla_s G + \mathbf{n} \delta G) \\ &= \int_S dS \frac{1}{|\mathbf{r} - \mathbf{r}'|} \frac{dG}{dR} \mathbf{n}' \cdot \{(\mathbf{r} - \mathbf{r}') \cdot \nabla_s \mathbf{r} + [(\mathbf{r} - \mathbf{r}') \cdot \mathbf{n}] \mathbf{n}\} \delta r \\ &= \int_S dS \frac{\mathbf{n}' \cdot (\mathbf{r} - \mathbf{r}')}{|\mathbf{r} - \mathbf{r}'|} \frac{dG}{dR} \delta r = \int_S dS \frac{\mathbf{e}_2' \cdot [(\mathbf{r} - \mathbf{r}') \wedge \mathbf{e}_1']}{|\mathbf{r} - \mathbf{r}'|} \frac{dG}{dR} \delta r \end{aligned} \quad (\text{A3})$$

where we have used the surface divergence theorem regarding closed surfaces. Before carrying out the functional derivatives of  $F_i$ , we firstly note

$$\delta \tilde{\gamma}(\mathbf{n}) = \tilde{\gamma}(\mathbf{n} + \delta \mathbf{n}) - \tilde{\gamma}(\mathbf{n}) = -\nabla_s \delta r \cdot \nabla_{s'} \tilde{\gamma}, \quad (\text{A4})$$

where  $\nabla_{s'} = \mathbf{e}_i \partial_{\zeta_i}$ . Then we can obtain

$$\begin{aligned} \delta \int_S dS \tilde{\gamma} &= \int_S dS [-\nabla_s \delta r \cdot \nabla_{s'} \tilde{\gamma} + \tilde{\gamma} (\nabla_s \cdot \mathbf{n}) \delta r] = \int_S dS [-\nabla_s \delta r \cdot (\nabla_{s'} \tilde{\gamma} + \mathbf{n} \tilde{\gamma}) + \tilde{\gamma} \nabla_s \cdot (\mathbf{n} \delta r)] \\ &= \int_S dS [\nabla_s \cdot (\nabla_{s'} \tilde{\gamma} + \mathbf{n} \tilde{\gamma})] \delta r - \int_S dS \nabla_s \cdot [(\nabla_{s'} \tilde{\gamma} + \mathbf{n} \tilde{\gamma}) \delta r] = \int_S dS [\nabla_s \cdot (\nabla_{s'} \tilde{\gamma} + \mathbf{n} \tilde{\gamma})] \delta r \\ &= \int_S dS [\tilde{\gamma}_{ani} + (\kappa_1 + \kappa_2) \tilde{\gamma}] \delta r. \end{aligned} \quad (\text{A5})$$

The functional derivatives from Eq. (36) can be found in Ref. [19]

$$\delta \int_S dS (3H^2 - K) = \int_S dS (3\Delta_s H + 2H^3 - 2HK) \delta r. \quad (\text{A6})$$

## Appendix B

Following the method as developed in Ref. [22], a local coordinate for the interface, with the  $z$  axis parallel to the normal  $\mathbf{n}$ ,  $x$  and  $y$  along the principal curvatures in the tangent plane, is firstly described as

$$z(x, y) = \frac{1}{2} (\kappa_1 x^2 + \kappa_2 y^2). \quad (\text{B1})$$

Then the element of the interface area is  $dS = \sqrt{g} dx dy$  with  $g = 1 + \kappa_1^2 x^2 + \kappa_2^2 y^2$ . It is easy to obtain  $\mathbf{n}' \cdot \mathbf{n} = g^{-1/2}$ . The tangent plane is also described by polar coordinates with  $x = r \cos \theta$  and  $y = r \sin \theta$ . Thus,  $F_f$  is first approximately evaluated by  $\mathbf{r}$  integral over the whole tangent plane

$$\begin{aligned} \int_S dS' \mathbf{n}' \cdot \mathbf{n} G &= \int_S dx dy G = \int_0^{2\pi} \int_0^{+\infty} d\theta dr \frac{r}{4\pi \sqrt{r^2 + z^2}} \exp(-\omega \sqrt{r^2 + z^2}) \\ &= \frac{1}{4\pi} \int_0^{2\pi} \int_0^{+\infty} d\theta dr \left( 1 - \frac{z^2}{2r^2} (1 + \omega r) \right) \exp(-\omega r) + O((\omega \kappa_i)^4) \\ &= \frac{\omega}{2} \left[ 1 - \frac{1}{2} \omega^2 (3H^2 - K) \right] + O((\omega \kappa_i)^4). \end{aligned} \quad (\text{B2})$$

## References

- [1] M.C. Cross, P.C. Hohenberg, *Rev. Mod. Phys.* 65 (1993) 851.
- [2] K.J. Lee, W.D. McCormick, Q. Ouyang, H.L. Swinney, *Science* 261 (1993) 189.
- [3] A. Hagberg, E. Meron, *Chaos* 4 (1994) 477.
- [4] P. Coulet, J. Lega, B. Houchmanzadeh, J. Lajzerowicz, *Phys. Rev. Lett.* 65 (1990) 1352.
- [5] R.E. Goldstein, D.J. Muraki, D.M. Petrich, *Phys. Rev. E* 53 (1996) 3933.
- [6] D.M. Petrich, R.E. Goldstein, *Phys. Rev. Lett.* 72 (1994) 1120.
- [7] Z.Z. He, J. Liu, *Phys. Rev. E* 79 (2009) 026105.
- [8] A. Mikhailov, *Phys. Rev. E* 49 (1994) 5875.
- [9] M. Bar, A. Hagberg, E. Meron, U. Thiele, *Phys. Rev. E* 62 (2000) 366.
- [10] Z.Z. He, J. Liu, *Europhys. Lett.* 85 (2009) 18003.
- [11] G.B. McFadden, A.A. Wheeler, R.J. Braun, S.R. Coriell, R.F. Sekerka, *Phys. Rev. E* 48 (1993) 2016.
- [12] A.A. Wheeler, G.B. McFadden, *Eur. J. Appl. Maths* 7 (1996) 367.
- [13] M. Monine, L. Pismen, M. Bar, M. Or-Guil, *J. Chem. Phys.* 117 (2002) 4473.
- [14] A. Makeev, M. Hinz, R. Imbuhl, *J. Chem. Phys.* 114 (2001) 9083.
- [15] N. Gottschalk, F. Mertens, M. Bar, M. Eiswirth, R. Imbuhl, *Phys. Rev. Lett.* 73 (1994) 3483.
- [16] F. Mertens, R. Imbuhl, *Nature* 370 (1994) 124.
- [17] H. Shoji, K. Yamada, D. Ueyama, T. Ohta, *Phys. Rev. E* 75 (2007) 046212.
- [18] A. Malevanets, R. Kapral, *Phys. Rev. Lett.* 77 (1996) 767.
- [19] H. Naito, M. Okuda, Z.-c. Ou-Yang, *Phys. Rev. E* 52 (1995) 2095.
- [20] B.C. Brower, D.A. Kessler, J. Koplik, H. Levine, *Phys. Rev. A* 29 (1984) 1335.
- [21] A.T. Dorsey, *Ann. Phys.* 233 (1994) 248.
- [22] B. Duplantier, R.E. Goldstein, V.V. Romero-Rochin, A.I. Pesci, *Phys. Rev. Lett.* 65 (1990) 508.